Carbohydrate Polymers 101 (2014) 471–478

Contents lists available at ScienceDirect

Carbohydrate Polymers

journal homepage: www.elsevier.com/locate/carbpol

Surface grafting of cellulose nanocrystals with poly(3-hydroxybutyrate-co-3-hydroxyvalerate)

Hou-Yong Yu[a,b,c,*], Zong-Yi Qin[b,**]

[a] The Key Laboratory of Advanced Textile Materials and Manufacturing Technology of Ministry of Education, College of Materials and Textile, Zhejiang Sci-Tech University, Hangzhou 310018, China
[b] State Key Laboratory for Modification of Chemical Fibers and Polymer Materials, College of Materials Science and Engineering, Donghua University, Shanghai 201620, China
[c] National Engineering Lab of Textile Fiber Materials & Processing Technology, Zhejiang Sci-Tech University

ARTICLE INFO

Article history:
Received 26 July 2013
Received in revised form 18 August 2013
Accepted 14 September 2013
Available online 23 September 2013

Keywords:
Cellulose nanocrystals
Poly(3-hydroxybutyrate-co-3-hydroxyvalerate)
Graft copolymers
Thermal property
Hydrophobic property

ABSTRACT

Chemically modified cellulose nanocrystals (CNCs) were synthesized by grafting poly(3-hydroxybutyrate-co-3-hydroxyvalerate) (PHBV) onto CNCs via homogeneous acylation reaction between N,N-dimethyl formamide (DMF) by using toluene diisocyanate (TDI) as coupling agent and dibutyltin dilaurate as catalyst. The resulting copolymers were studied by using ^{1}HNMR, FT-IR, WAXD, DSC, TGA and contact angle measurements. Results showed that the copolymers kept their initial morphological integrity. Moreover, it is found that with the increase of the TDI/PHBV fractions, two transition exhibitions occurred in their thermal and hydrophobic properties, which could be modulated through controlling the lengths and grafting densities of PHBV side chains. Compared with those of neat PHBV, the crystallization of PHCN7 became easy while the crystallinity slightly decreased to 55.5%, the maximum decomposition temperature increased by 48.5 °C, meanwhile the contact angle increased to 58° as compared to neat CNCs (30°).

1. Introduction

Cellulose nanocrystals (CNCs) derived from renewable cellulose resources, have been used as green reinforcing agent in bionanocomposites by virtue of their advantages of high Young's modulus (150 GPa) and strength (10 GPa), biodegradability, biocompatibility, non-toxicity, renewability, and easy chemical modification due to abundant hydroxyl groups. It is well known that the dispersion state of the hydrophilic CNCs into a hydrophobic polymer matrix play an important role in enhancing polymer composites (Habibi, Lucia, & Rojas, 2010; Klemm et al., 2011; Yu, Qin, Liu, et al., 2012; Yu et al., 2013). However, the CNCs produced by the common method (sulfuric acid hydrolysis) exhibit poor thermal stability with low maximum degradation temperature (T_{max}) of 250 °C, which would further prevent their processing by using several melt processing techniques such as injection molding, twin-screw compounding and extrusion (Yu et al., 2013). On the other hand, due to their high surface area and hydrophilic nature, both intermolecular and intramolecular hydrogen bonding of CNC hydroxyl groups cause the nanocrystals to self-aggregate easily, leading to low efficiency of reinforcement in nanocomposites (Viet et al., 2007; Yu, Qin, Liu, et al., 2012). Therefore, the hydrophilic CNCs are immiscible with hydrophobic polymer matrices. A potential solution for reducing the reactivity of its surface hydroxyl groups by surface chemical modification is required. Indeed, more hydroxyl groups on each glucose chains of CNCs would offer various possible coupling reaction sites. Recently, more efforts to promote hydrophobicity of CNCs have been reported, involving the use of surfactants (Menezes et al., 2009), castor oil (Shang et al., 2013), silane agent (Taipina, Ferrarezi, Yoshida, & Gonçalves, 2013), acetylation (Lin, Huang, & Chang, 2011; Wang et al., 2013), stearic acid chloride (Thielemans, Belacem, & Dufresne, 2006), phenyl isocyanate (Angellier, Molina-Boisseau, Belgacem, & Dufresne, 2005) and polycaprolactone (Chen, Dufresne, Huang, & Chang, 2009; Chen, Cheng, & Xu, 2009; Habibi et al., 2008; Habibi & Dufresne, 2008; Lönnberg, Fogelström, Azizi-Samir, Malmström, & Hult, 2008) and other polymer grafting (Enomoto-Rogers, Yoshinaga, & Takano, 2011; Wang et al., 2012). Moreover, it is found that there are more advantages for grafting high molecular weight polymers on CNC surfaces than low molecular weight moieties because high enough molecular weight polymer chains grafted on the CNCs can enhance greatly thermal and mechanical properties

* Corresponding author at: The Key Laboratory of Advanced Textile Materials and Manufacturing Technology of Ministry of Education, College of Materials and Textile, Zhejiang Sci-Tech University, Hangzhou 310018, China. Tel.: +86 571 86843618; fax: +86 571 86843619.
** Corresponding author.
E-mail addresses: phdyu@zstu.edu.cn (H.-Y. Yu), phqin@dhu.edu.cn (Z.-Y. Qin).

0144-8617/$ – see front matter © 2013 Elsevier Ltd. All rights reserved.
http://dx.doi.org/10.1016/j.carbpol.2013.09.048

of the nanocomposites due to entanglements between grafted and ungrafted chains (Habibi et al., 2008; Habibi & Dufresne, 2008). From above, in order to improve reinforcement efficiency of CNCs in nanocomposites as well as its thermal stability, surface grafting hydrophobic polymer on the CNCs as a compatibilizing tail might be a good choice.

Bacterially synthesized poly(3-hydroxybutyrate-co-3-hydroxyvalerate) (PHBV) have attracted great scientific and technological interests due to their important applications, such as environmentally friendly bioplastics, tissue engineering scaffolds, wound dressings, temporary prostheses, and controlled/sustained release drug delivery vehicles and so on. It also shows good biocompatibility, nontoxicity, and compatibility with tissue and blood (Chen et al., 2009; Chen, Cheng, et al., 2009; Chen & Wu, 2005; Hu, Wei, Zhao, Liu, & Chen, 2009; Ke, Wang, Renb, Zhao, & Huang, 2010; Yu, Qin, Wang, & Zhou, 2012). However, there are several shortcomings for the commercial use of the PHBV generally with less than 15 mol% fraction of hydroxyvalerate (3HV), such as rigidity and brittleness caused by high crystallinity, poor thermal stability, and narrow processing window (Liu, Zhu, Wu, & Qin, 2009; Yu, Qin, Wang, et al., 2012). On the other hand, PHBV films or fibers will usually stick to themselves during melt processing due to its slow crystallization rate. Therefore, some improvements on the crystallization behavior and thermal stability of PHBV was frequently carried out through judicious selection of some biocompatible materials with specific chemical modification for controlling chemical structures, further obtaining the expected thermal properties and so on (Chen et al., 2009; Chen, Cheng, et al., 2009; Lao, Renard, Linossier, Langlois, & Vallée-Rehel, 2007; Li et al., 2009; Yu, Qin, Wang, et al., 2012).

In this work, a new approach was presented to prepare novel biodegradable graft copolymers combining the advantages of CNCs backbone and hydrophobic PHBV side chains, which can improve the hydrophobicity of CNCs and thus promote the desirable compatibility with hydrophobic polymer matrices. Moreover, the effect of different lengths and grafting densities of PHBV side chains on crystallization behavior, thermal and hydrophobic properties of the resulting copolymers were investigated. The purpose was to study these properties of the copolymers, in order to select hydrophobic copolymer with high thermal stability for enhancing the PHBV matrix in a final nanocomposite. Nanocomposites will be prepared in a continuation of this work.

2. Experimental

2.1. Materials

PHBV ($M_n = 5.90 \times 10^4$, $M_w = 1.58 \times 10^5$, and the molar ratio of HV is 2.57%) was obtained from Tiannan Biological Material Co., Ltd. (Ningbo, China) and purified by reprecipitation in methanol from chloroform solutions. Commercial microcrystalline cellulose (MCC, particle size: about 20 μm), toluene diisocyanate (TDI), ethanol (99.8%), diglyme, N,N-dimethyl formamide (DMF), chloroform, ethylene glycol, dibutyltin dilaurate (90.0%), hydrochloric acid (HCl), ammonia solution ($NH_3 \cdot H_2O$), petroleum ether and $CaCl_2$ were purchased from the Shanghai Guoyao Group Chemical Reagent Co., Ltd. (Shanghai, China). All reagents and solvents were used as received or purified using standard procedures.

2.2. Synthesis of PHCN copolymers

The details for preparing the cellulose nanocrystals (CNCs) have been given in elsewhere (Yu et al., 2013). The CNC aqueous suspension was prepared by mild acid hydrolysis of the MCCs in the hydrothermal kettle at 110 °C for 3 h, following by ammonia

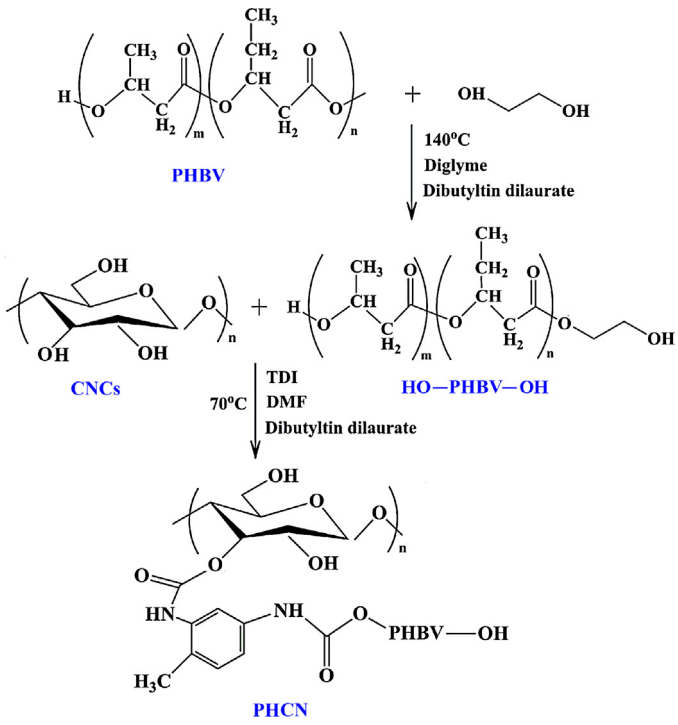

Scheme 1. Synthesis of PHCN copolymer.

neutralization, and then was heated at 100 °C for 1 h to remove the residual ammonium groups. After 10 min of exposure to ultrasonic irradiation, the CNC suspension was freeze-dried for 48 h to obtain the dry CNCs.

Telechelic OH-terminated PHBV oligomers (denoted as HO – PHBV – OH) were prepared by a transesterification procedure as our previously reported method (Liu et al., 2012; Yu, Qin, Wang, et al., 2012), and the reaction was illustrated as shown in Scheme 1. The detailed synthesis process was as follows: 30 g PHBV and 300 mL of diglyme were placed in a four-necked round bottom flask under nitrogen atmosphere. Then the flask was heated to 140 °C in an oil bath with continuously mechanical stirring. After PHBV was dissolved completely, 60 mL of ethylene glycol and dibutyltin dilaurate (0.3 g) as catalyst were added to the flask. After a desired reaction time of 7.5 h, the products were precipitated with ethanol, washed repeatedly with ethanol, and dried under vacuum. The molecular weight of HO—PHBV—OH was about 1980 g mol^{-1} by measuring Gel permeation chromatography (Liu et al., 2012; Yu, Qin, Wang, et al., 2012).

Grafting PHBV onto the surface of CNCs through the esterification reaction between hydroxyl groups of the CNCs and hydroxyl groups of HO—PHBV—OH by using toluene diisocyanate (TDI) as coupling agent via the synthetic pathway was shown in Scheme 1. The grafting conditions, such as the reaction time, temperature and mass ratio of PHBV oligomer to CNCs, were optimized to obtain the maximum grafting percentage (GP%). The PHBV/CNC mass ratio can be optimized according to the number of functional groups, but it did not mean that all the PHBV could be successfully grafted onto the CNCs. It is found that the larger grafting percentage can be achieved for the PHBV/CNC ratio of 4:1 (346%) with the TDI/PHBV fraction of 7 than those for the PHBV/CNC ratio of 6:1 (342%) and 2:1 (335%) under similar reaction conditions. Hence, the PHBV/CNC mass ratio was chosen to be 4:1 in this work, and the effects of the TDI/PHBV fractions on structures of the PHCN copolymers were further studied. The detailed synthesis process was as follows: The CNC suspension (about 1.0 g) and 80 mL of anhydrous DMF were added into a 250 mL four-neck flask with a mechanical stirrer,

nitrogen inlet and outlet. Then the flask was heated to 90 °C in an oil bath with mechanical stirring. After any trace water of the stirred mixture was removed through azeotropic distillation, only 50 mL of DMF remained in the flask. When the flask was cooled to 70 °C, various TDI fractions and ten drops of dibutyltin dilaurate were sequentially added into the flask for 1 h under a nitrogen atmosphere. Subsequently, 4.0 g PHBV oligomers were added to the flask with continuously mechanical stirring. After a desired reaction time of 48 h, the resulting products were redissolved into chloroform to remove the crosslinked substances and then precipitated by using a mixture of anhydrous alcohol and petroleum ether twice to remove the catalyst. Finally, the ungrafted PHBV in the copolymers could be removed by using soxhlet extractor. The product was wrapped by a filter paper, and then soaked in the chloroform (as extracting agent). This purified process was similar as the preparation process of PHBV-graft-chitin nanocrystals (Wang et al., 2012). Then the ungrafted PHBV was removed after reflux condenser with chloroform for 12 h. after vacuum-drying at 40 °C, the pure copolymers could be obtained and designated as PHCN*x*, where *x* denoted the TDI/PHBV fractions (molar ratio). The tested films for static contact angle test were prepared by dissolving the copolymer in chloroform (10 wt%) and cast into thin sheets.

The grafting yield was recorded to calculate the grafting percentage (GP%), grafting efficiency (GE%) and weight conversion (WC%) according to the following equation:

$$GP\% = \frac{(m_C - m_{CNC})}{m_{CNC}} \times 100 \quad (1)$$

$$GE\% = \frac{(m_C - m_{CNC})}{m_{PH}} \times 100 \quad (2)$$

$$WC\% = \frac{m_C}{m_{PH}} \times 100 \quad (3)$$

where m_C, m_{CNC} and m_{PH} were the weights of extract graft product, CNCs, and PHBV, respectively.

2.3. Characterization

The morphologies of CNCs and PHCN7 were observed on a field emission scanning electron microscopy (FE-SEM, HITACHI S-4800) at 5.0 kV. The ^{1}H NMR spectra of PHBV and the resulting copolymers were obtained from a Bruker Avance 400 NMR spectrometer in 5 mm tubes with $CDCl_3$ as a solvent at room temperature.

FT-IR spectra were recorded on a Nicolet 8700 FT-IR spectrophotometer. Each spectrum was collected with 64 scans and 2 cm^{-1} resolution at room temperature.

Wide-angle XRD measurements (WAXD) were carried out on a RIGAKU D/Max-2550 PC diffractometer with an area detector operating under Cu Kα (1.5418 Å) radiation (40 kV, 40 mA) at room temperature. All the samples stood for 2 weeks at room temperature to reach equilibrium crystallization before measuring.

DSC measurements of PHBV and the resulting copolymers were performed on MDSC TA-2910 differential scanning calorimeter by employing a 40 mL min^{-1}, flow of dry nitrogen as a purge gas for the sample and reference cells. The sample was firstly heated from room temperature to 200 °C at a rate of 20 °C/min, and kept at 200 °C for 5 min to eliminate the previous thermal history. Subsequently, the sample was cooled to 0 °C at a rate of 10 °C/min, and heated again to 200 °C at a rate of 10 °C/min. Main thermal parameters were obtained from DSC curves, such as melt crystallization temperature (T_{mc}), melt crystallization enthalpies (ΔH_{mc}), cold crystallization temperature (T_{cc}), cold crystallization enthalpies (ΔH_{cc}), melting temperature (T_{m1}, T_{m2}), melting enthalpies (ΔH_m).

TGA was carried out using Netzsch TG209 F1 TGA instrument coupled with QMS. The samples were heated at 10 °C/min from room temperature to 600 °C in a dynamic nitrogen atmosphere with the flow rate of 30 mL min^{-1}.

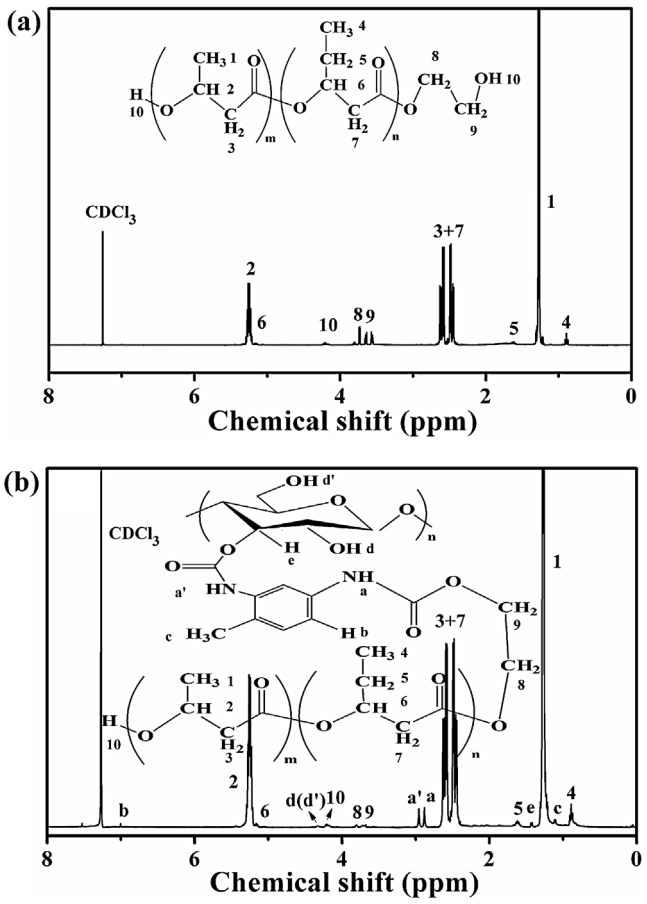

Fig. 1. ^{1}H NMR spectra of OH-terminated PHBV oligomer (a) and PHCN7 copolymer (b).

The contact angles of the neat PHBV, CNCs and the resulting copolymer were measured on the air surface of their films using pendant drop method on a Dataphysics OCA40 contact angle analyzer at room temperature. About 2 μL of deionized water was dropped onto the surface at a contact time of 5 s. Twenty independent determinations at different sites of the sample were averaged.

3. Results and discussion

3.1. Chemical structure: ^{1}H NMR spectra

^{1}H NMR spectra were used to verify the formation of the graft copolymers as shown in Fig. 1. The ^{1}H NMR spectra of OH-terminated PHBV oligomer and PHCN7 copolymer (as an example of copolymers) were investigated. As shown in Fig. 1(a), the strong peaks at 1.27 and 5.26 ppm, and weak peaks at 0.89 and 5.21 ppm were attributed to the terminal methylene protons (H_1, H_4) and the internal methylene protons (H_2, H_6) of PHBV side chain, respectively. Moreover, the peak at 4.20 was assigned to the terminal hydroxyl protons (—CH_2—OH, H_{10}), which was formed during the transesterification reaction for preparing telechelic OH-terminated PHBV(Chen et al., 2009; Chen, Cheng, et al., 2009; Yu, Qin, Wang, et al., 2012). In Fig. 1(b), all the characteristic peaks of PHBV and CNCs can be found in the spectra of the copolymers. The peaks at 1.42 ppm and around 4.32–4.39 ppm were assigned to the —CH proton (H_e) of glucose unit and the —OH protons (H_d and $H_{d'}$) of CNC backbone (Tehrani & Neysi, 2013). More importantly, new peaks at 1.12 and 7.00 ppm, and multiple peaks around 2.86–2.95 ppm

were belonged to the protons of methyl group and the benzene ring, —NH—COO from TDI, indicating that the graft copolymers were successfully prepared. Subsequently, the degree of polymerization of PHBV (DP) and the degree of substitution of copolymer (DS), and the number average molecular weight ($M_{n,NMR}$) of the copolymer can be calculated by peak intensity from ^{1}H NMR spectra to speculate graft structures of the copolymers, respectively.

$$DP = \left(\frac{I_d + I_1}{I_d}\right) \quad (4)$$

$$DS = \left(\frac{2 \times I_{10}}{3 \times I_d}\right) \quad (5)$$

$$M_{n,NMR} = DS \times DP \times 1980 \quad (6)$$

where I_1, I_{10} and I_d are the integral peak areas of methylene and terminal hydroxyl groups of PHBV oligomers, and hydroxyl groups of CNCs, respectively. Further, 1980 g mol^{-1} is the molecular weight of telechelic OH—terminated PHBV oligomers (Liu et al., 2012; Yu, Qin, Wang, et al., 2012).

Table 1 summarized the grafting parameters (GP%, GE% and WC%), the structure parameters (DS and DP), and the molecular weight ($M_{n,NMR}$) for the copolymers prepared at the different TDI/PHBV fractions. When the fractions changed from 1 to 8, the values of GP%, GE% and WC% almost progressively increased from 215%, 53.8% and 78.8% to 374%, 93.5% and 118.5%, respectively. However, for the TDI/PHBV fraction of 10, these values decreased to 366%, 91.5% and 116.5%, respectively. Similar change trends for $M_{n,NMR}$ and DS can be found, whereas the DP increased gradually with the TDI/PHBV fractions. These results indicated that the hydroxyl groups of the CNC could effectively initiated graft polymerization with PHBV segments via the TDI coupling agent. On the one hand, the isocyanate groups of TDI grafted on CNCs would link to hydroxyl groups of PHBV, which determine the grafting density. On the other hand, TDI isocyanate groups of PHBV graft side chains were also active in connecting PHBV oligomers, which determine the length of side chains. There exists a competition balance between terminal hydroxyl groups of PHBV side chains and CNC surface hydroxyl groups to initiate polymerization with PHBV oligomers. When the graft side chains was long enough, the terminal hydroxyl groups of PHBV side chains could not initiate graft polymerization due to the strong excluded volume effects of adjacent long chains, and thus PHBV oligomers would be grafted onto CNCs, resulting in relatively short side chains in the copolymers as well as broad length distribution. It is well known that the lengths and the grafting density of graft side chains can be determined by the DP and DS values of the copolymers, respectively (Yu, Qin, Wang, et al., 2012; Zhu, Dong, Wang, & Wang, 2010). From above, with the increase of the TDI/PHBV fraction, a transition exhibition occurred in the DP and DS values. When the TDI/PHBV fraction was below 7, terminal hydroxyl groups of PHBV side chains was more active than the hydroxyl groups of CNC surface, so the PHBV side chains would graft new PHBV oligomers to mainly form the copolymers with more long side chain. When the TDI/PHBV fraction was at 8 or 10, the addition of more TDI would break competition balance between the terminal hydroxyl groups of PHBV side chains and the hydroxyl groups of CNC surface. Both PHBV side chains and CNCs would connect new PHBV oligomers, leading to the occurrence of short side chains and broad length distribution in the copolymers (such as PHCN8 and PHCN10). However, the TDI/PHBV fraction of 10, although more short side chains appeared, the short side chains would became long due to the addition of much more TDI. It indicated that the side-chain length and grafting density of the copolymers could be adjusted through changing the TDI/PHBV fractions. With the increase of the TDI/PHBV fractions, the grafting structure of the copolymers might change from relatively long side chain with low grafting density, to more long side chain with relatively high grafting density, and then broad length distribution and high grafting density, finally relatively narrow length distribution and high grafting density.

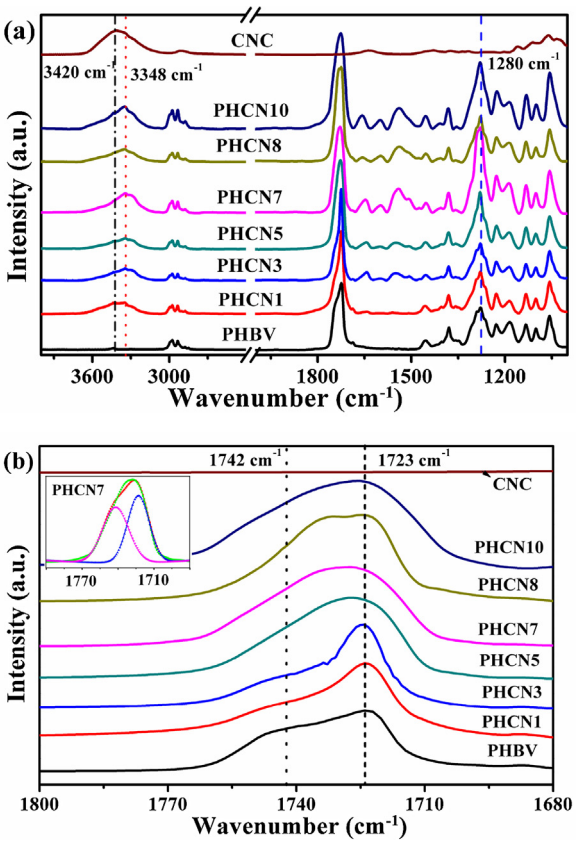

Fig. 2. FT-IR spectra (a) and carbonyl stretching region (C=O) in the infrared spectra (b) of neat PHBV, CNCs and the resulting copolymers prepared under various TDI/PHBV fractions and PHCN7 copolymer (insert).

3.2. Chemical structure: FT-IR spectra

Fig. 2(a) shows the FT-IR spectra of neat PHBV, CNC and the resulting copolymers prepared under various TDI/PHBV fractions. All the characteristic peaks of PHBV and CNCs appeared in the FT-IR spectra of the copolymers. For example, the broad bands in the 3420 and 2900 cm^{-1} were assigned to O—H stretching vibrations and C—H stretching vibrations modes of CNCs, respectively (Chen et al., 2009; Chen, Cheng, et al., 2009; Taipina et al., 2013; Yu, Qin, Liu, et al., 2012). The bands at 1280, 1456, 1723, 2930 and 2979 cm^{-1} were attributed to stretching vibration of —C—O—C—, bending modes of the C—H, stretching vibration of C=O in ester, and symmetric and asymmetric stretching vibration of CH_3 of PHBV, respectively (Liu et al., 2009; Yu, Qin, Liu, et al., 2012; Yu, Qin, Wang, et al., 2012). Compared with that of CNCs, the intensity of O—H stretching for the glucose rings of CNCs from the copolymers around 3420 cm^{-1} decreased obviously, implying the hydroxyl groups of CNCs were consumed in reaction with hydroxyl groups of PHBV oligomers through TDI as the coupling agent. Moreover, three new bands appeared at 3348, 1660 and 1542 cm^{-1} can be contributed to the symmetric stretching vibration and medium bending vibration of N—H from imino group (—OOCNH—) of polyurethane linkage, respectively. This implied the PHCN copolymers was successfully prepared by using TDI as the coupling agent. In this case, the peaks at 1602 and 1453 cm^{-1} related to aromatic groups were also the strong evidence in the

Table 1
The grafting parameters, structure parameters and number average molecular weight for the resulting copolymers prepared under various TDI/PHBV fractions.

Sample	GP%	GE%	WC%	DP[a]	DS[a]	$M_{n,NMR}$(g mol^{-1})[a]
PHCN1	215	53.8	78.8	20.2	0.54	21,597.8
PHCN3	252	63.0	88.0	25.6	0.62	31,426.6
PHCN5	298	75.4	99.5	26.8	0.66	35,022.2
PHCN7	346	86.5	111.5	32.5	0.72	46,332.0
PHCN8	374	93.5	118.5	37.8	0.86	64,365.8
PHCN10	366	91.5	116.5	39.4	0.82	63,969.8

[a] DP, DS and $M_{n,NMR}$ is determined by ^{1}H NMR spectroscopy.

presence of TDI. Furthermore, an increase in the intensity of some characteristic bands for PHBV occurred with the increasing of the TDI/PHBV fractions as shown in Fig. 2(b), such as the increase in the bands at 2930 and 2979 cm^{-1} belonging to the CH_3 stretching vibration from side pendant alkyl groups of PHBV. This indicated an increasing content of PHBV in the copolymers with the increase of the TDI/PHBV fractions. In addition, as the TDI/PHBV fractions increased, the intensity of crystalline–sensitive peaks at 1280 cm^{-1} (C—O—C stretching mode) of the copolymers increased gradually, and then decreased. The strongest peak intensity appeared in PHCN7, indicating its crystalline components were higher than other copolymers.

To better evaluate the graft length of PHBV side chains on crystallization of PHCN copolymers, IR spectra of the carbonyl band in the range from 1680 and 1800 cm^{-1} were curve-fitted by using Gauss/Lorentz spectral function. As shown by the insert presented in Fig. 2(b), the band at 1723 cm^{-1} and its shoulder at 1742 cm^{-1} were related to the crystalline and amorphous components in PHBV, respectively (Lao et al., 2007; Sato et al., 2004; Yu, Qin, Wang, et al., 2012). Thus, the area ratio of the bands situated at 1742 and 1723 cm^{-1} (A_{1742}/A_{1723}) can be calculated as listed in Table 2. With the increase of the TDI/PHBV fractions, the A_{1742}/A_{1723} values decreased greatly from 1.36 for PHCN1 to 1.01 for PHCN7, and then increased to 1.05 for PHCN8, finally reduced to 0.98 for PHCN10. It indicated the crystalline components were increased gradually, except that slight decrease appeared in the PHCN8. It is well known that the mobility of long side chains for linear polymer is easier than relatively short one (Yu, Qin, Wang, et al., 2012; Zhu et al., 2010). However, the strong spacial restriction and even entanglement between long side-chains with high grafting density were usually appeared in the copolymers, thus the mobility of crystalline PHBV chains would be restricted. Therefore, for those copolymers with long PHBV side chains, such as PHCN7 have more crystalline domains, whereas the copolymers (PHCN8) with relatively broad length distribution and more short side chains contributed to larger amorphous domains. When the TDI/PHBV fraction increased to 10, A_{1742}/A_{1723} values decreased, implying the increase of crystalline components in the PHCN10 due to relatively narrow graft length distribution.

3.3. Crystal structure: WAXD

The crystal structures of neat PHBV, CNCs and the nanocomposites were studied by WAXD, and the diffraction patterns were illustrated in Figure S1. The CNCs showed four characteristic cellulose I reflections, the diffraction peaks at 14.6°, 16.4°, 22.6° and 34.0° were assigned to (1$\bar{1}$0), (110), (200) and (004) planes of cellulose Iβ, respectively (Enomoto-Rogers et al., 2011; Shang et al., 2013; Taipina et al., 2013; Yu et al., 2013). The peaks at 13.3°, 16.8°, 19.5°, 21.1°, 21.4°, 25.6°, 27.2° and 29.9° were assigned to (020), (110), (021), (101), (111), (121), (040) and (002) planes of PHBV, respectively, and the unit cells of 3HB and 3HV in PHBV belonged to the orthorhombic crystal system (Bluhm & Hamer, 1986; Sato et al., 2004; Yu, Qin, Wang, et al., 2012). The diffraction peaks of CNCs were not observed in the WAXD patterns of the copolymers, attributing to the surface of CNCs covered with a semicrystalline shell organized by grafted PHBV segments chains, which was supported by comparing morphology of CNCs and PHCN copolymer (in Figure S2). In addition, it is found that the rod-like shape of PHCN7 (as an sample of the copolymers) was preserved, but its size was slightly increased compared to neat CNCs. Similar phenomenon was found in the grafting PCL or silane agents on the CNCs (Chen et al., 2009; Chen, Cheng, et al., 2009; Taipina et al., 2013). These similar peaks of PHBV appeared in the diffraction patterns of the copolymers, suggesting that the crystal structure of PHBV segments was essentially preserved and the longer side chains facilitated formation of the ordered crystalline arrangement. Further, two transitions in the intensity for the (021), (101) and (200) planes can be observed. It is found that the intensities gradually increased with the increase of the TDI/PHBV fraction from 1 to 7, then decreased for 8, and finally increased for 10. It has been reported that the increase in the intensity of (200) peak could be contributed to the preferential growth of PHBV crystals along the direction of the α axis (Bluhm & Hamer, 1986). Therefore, the crystal growth of PHBV (in the copolymers with long side chains) along the direction of α axis was enhanced, but restricted in the copolymers with broad length distributions.

Table 2 listed the crystallinity (X_c) of neat PHBV, CNCs and the resulting copolymers. It can be seen that X_c of the copolymers were lower than 58.1% for neat PHBV and CNCs. This can be ascribed to the confined movements of the PHBV side chains due to the spacial restrictions, resulting in the decrease of the X_c. With the increase of the TDI/PHBV fractions, the X_c of the copolymers increased gradually from 50.3% for PHCN1 to 55.5% for PHCN7, and then decreased to 48.1% for PHCN8, finally increased to 49.4% for PHCN10. The decrease in X_c implied that relatively broad length distribution and high grafting density of PHBV side chain appeared in the copolymer, which induced the crystal imperfection mainly due to interference of the short chain length of PHBV segments. However, for PHCN10, more long side chain with relatively narrow length distribution of PHBV segments would give more fluidity and be easily prone to crystallize. Therefore, two significant transitions in the X_c can be observed.

3.4. Crystallization behavior: DSC

The degradation of biopolyesters began in the amorphous zone and then the crystalline zone. The degree of crystallinity plays an important role in the physical properties and biodegradability of biodegradable polymers. Fig. 3 shows the DSC curves of neat PHBV and the resulting copolymers during first cooling and second heating processes, and the corresponding thermal parameters are listed in Table 2. As shown in Fig. 3(a), no obvious melt crystallization peak appeared in the neat PHBV during the first cooling scans, whereas the cold crystallization peak can be found in the second heating scans. However, a strong crystallization peak could be observed for the copolymers with the TDI/PHBV fractions below 7, and the change in the crystallization behavior exhibited two significant transitions exhibition as shown in Fig. 3 (a) and (b). With the increasing of the TDI/PHBV fractions, the melt crystallization

Table 2
The A_{1742}/A_{1723} value, crystallinity and thermal parameters for neat PHBV, CNCs and the resulting copolymers under various TDI/PHBV fractions.

Sample	A_{1742}/A_{1723}[a]	X_c (%)[b]	T_{cc} (°C)	ΔH_{cc} (J/g)	T_{mc} (°C)	ΔH_{mc} (J/g)	T_{m1} (°C)	T_{m2} (°C)	ΔH_{m2} (J/g)	T_{max} (°C)
PHBV	2.25	58.1	41.2	56.1	–	–	111.7	130.7	74.7	245.6
PHCN1	1.36	50.3	–	–	51.3	52.2	109.6	132.8	54.7	285.6
PHCN3	1.17	52.5	–	–	67.7	54.0	129.6	143.2	58.8	287.7
PHCN5	1.10	53.2	–	–	76.1	55.9	135.3	146.7	60.2	288.5
PHCN7	1.01	55.5	–	–	77.9	56.7	136.5	150.8	65.8	294.1
PHCN8	1.05	48.1	53.5	33.9	–	–	134.3	149.5	45.2	292.7
PHCN10	0.98	49.4	41.0	36.2	28.2	8.1	114.7	138.9	49.3	294.3
CNC	–	88.6	–	–	–	–	–	–	–	363.9

[a] The ratio for the copolymers was calculated from the FT-IR spectra.
[b] X_c was calculated from the WAXD patterns.

peak became gradually stronger, and the melt crystallization temperature (T_{mc}) increased from 51.3 °C for PHCN1 to 77.9 °C for PHCN7, which indicated when the grafting density of PHBV side chains was high enough, the melt crystallization of the copolymers would be enhanced. Besides, the CNCs should have a positive effect on the crystallization of PHBV (such as the nucleation effect). When the TDI/PHBV fractions was at 8, no obvious melt crystallization peak appeared, only a cold crystallization temperature peak at 53.5 °C was observed. As the TDI/PHBV fractions increased to 10, the cold crystallization temperature (T_{cc}) decreased to 41.0 °C. It indicated that broad length distribution even with high grafting density was still resulted in relative difficulty for the crystallization of the copolymers due to the spacial restriction effect and entanglement between long side chains, and especially interference of the short and long PHBV side chains, thus the cold crystallization peak appeared. When the length distribution became narrower during the high TDI/PHBV fractions of 10, the crystallization of the copolymer became easy, so the T_{cc} shifted to lower temperature.

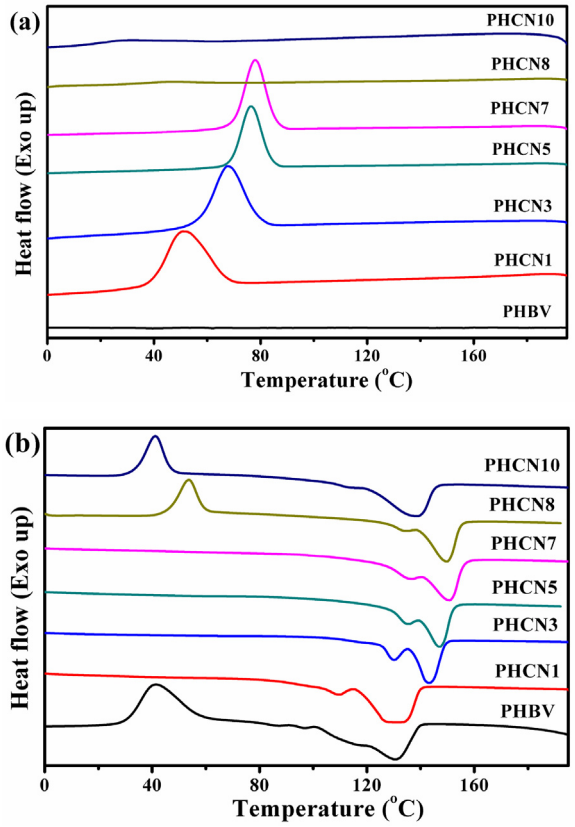

Fig. 3. DSC traces of neat PHBV and the resulting copolymers prepared under various TDI/PHBV fractions obtained during the first cooling (a) and second heating (b) scans at a rate of 10 °C/min.

Generally, the second heating run was used to measure the crystal structure formed during the non-isothermal crystallization. Therefore, the DSC curves of the second heating processes for neat PHBV and the resulting copolymers was illustrated in Fig. 3(b). The double melting peak located at 111.7 and 130.7 °C for neat PHBV can be formed through a melting, recrystallization and remelting process (Liu et al., 2009; Yu, Qin, Liu, et al., 2012; Yu, Qin, Wang, et al., 2012). Compared to neat PHBV, all the copolymers prepared at the different TDI/PHBV fractions exhibited similar double melting peaks, but their peak positions have great difference, which implied that the crystallization ability of copolymers was greatly affected by their grafting structures. Generally, the melting point from the relatively high temperature endotherm such as the second melting point (T_{m2}), was usually taken as the true melting temperature (T_m) for the copolymers (Liu et al., 2009; Yu, Qin, Wang, et al., 2012). It can seen from Table 2 that the T_{m2} of the copolymers with the TDI/PHBV fraction below 7 was higher than that of neat PHBV. With the TDI/PHBV fractions varied from 1 to 7, the T_{m2} of the copolymers shifted from 132.8 to 150.8 °C, and the heat of fusion (ΔH_m) increased from 54.7 to 65.8 J/g. As far as we know, the higher the DP and DS of the graft polymers, the higher the melting temperature and the heat of fusion (Yu, Qin, Wang, et al., 2012; Zhu et al., 2010). Once the TDI/PHBV fraction reached to 8, the T_{m2} decreased to 149.5 °C with ΔH_m of 45.2 J/g. This further supported that PHCN8 had the more boarder side-chain length distribution than other copolymers, the crystallization process of the short and long PHBV side chains would be interfered each other, resulting in the imperfection of PHBV crystals and thus the decrease in T_{m2}. For PHCN10, T_{m2} shifted to lower temperature with the relatively high ΔH_m of 49.3 J/g. This indicated longer side chains was indeed beneficial to induce entanglement between them and thus the decrease in the T_{m2} due to crystal imperfection. This was consistent with the NMR and WAXD results. From above, both T_m and X_c of the resulting copolymers can be adjusted by simply modulating the TDI/PHBV fractions to meet the requirements of medical applications.

3.5. Thermal stability: TGA

The effects of the length and grafting density of PHBV side chains on the thermal stability of the copolymers at the heating rate of 10 °C/min were studied as shown in Fig. 4, and the thermal parameters were summarized in Table 2. Thermal degradation through a one-step process can be observed, and the thermal stability of the copolymers was better than that for neat PHBV at 245.6 °C, but poorer than that for CNCs at 363.9 °C. This result can be ascribed to the covalent bond between PHBV chains and CNC backbone, and crystalline structures in the copolymers due to their different graft structures. Generally, the more the crystal perfection (crystallinity) of the copolymers, the better the thermal stability of the copolymers. Therefore, T_{max} exhibited similar trend as well as X_c (in Table 2). With the increase of TDI/PHBV fractions, T_{max} increased from 285.6 °C for PHCN1 to 294.1 °C for PHCN7, and then reduced

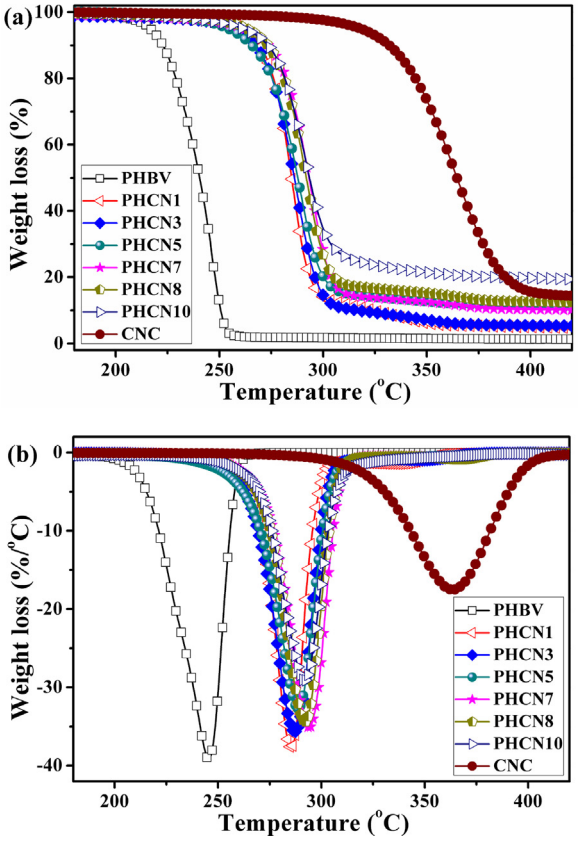

Fig. 4. The TGA (a) and DTG (b) curves of neat PHBV, CNCs and the resulting copolymers prepared under various TDI/PHBV fractions.

to 292.7 °C for PHCN8, finally increased to 294.3 °C for PHCN10. The decrease in the T_{max} can be attributed to the crystal imperfection that was mainly induced by the broad length distribution and a number of short PHBV side chains in copolymers. More short PHBV chains could impair its thermal stability, such as PHCN8. While more long side chains and relatively high grafting density were presented in the copolymer, such as PHCN7 and PHCN10, especially the T_{max} of PHCN7 increased by 48.5 °C compared to neat PHBV, indicating thermal stability of the copolymer can be enhanced significantly.

3.6. Hydrophobic property: contact angle measurement

The grafting hydrophobic PHBV on the CNC surfaces was expected to enhance the hydrophobicity of the CNCs for improving the interfacial interaction and thus miscibility with hydrophobic polymers. Static contact angle measurements were used to estimate the change in hydrophobicity of CNCs and the copolymer films as shown in Fig. 5. It can be observed that the copolymers have larger contact angle than 30° for neat CNCs, which can be attributed to the formation of the PHBV with hydrophobic pendant alkyl side chains wrapping of the CNCs. This was supported by the FT-IR and WAXD results. With the increase of the TDI/PHBV fractions, the contact angle of the copolymer gradually increased from 46° for PHCN1 to 58° for PHCN7, and then reduced to 55° for PHCN8, finally increased to 60° for PHCN10. Nevertheless, PHCN8 with more hydroxyl groups of short chains showed the slightly decreased contact angle. Among these copolymers, the PHCN10 showed the most hydrophobic with contact angle of 60°, which can be attributed to more long graft side chains with high grafting density under the high TDI/PHBV fractions.

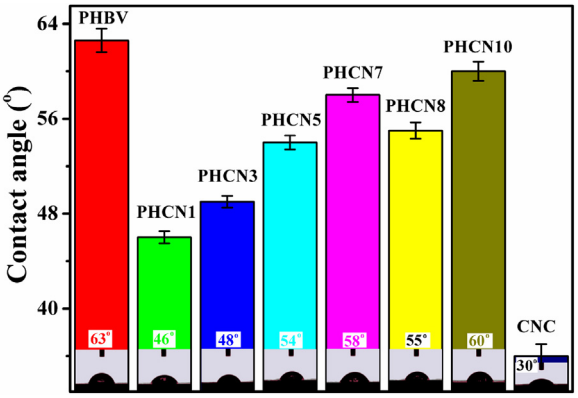

Fig. 5. The contact angles of neat PHBV, CNCs and the resulting copolymers prepared under various TDI/PHBV fractions.

4. Conclusions

A series of biodegradable PHCN copolymers were prepared through the homogeneous acylation reaction between CNCs and telechelic OH-terminated PHBV oligomer at a constant mass ratio of PHBV to CNCs of 4:1, in which TDI was used as coupling agent and dibutyltin dilaurate as catalyst. The crystallinity, melting temperature, thermal degradation temperature and hydrophobicity of the copolymers could be modulated through changing the TDI/PHBV fraction to control the length and grafting density of PHBV side chains. It is found that two transition exhibitions occurred on the crystallization and thermal degradation behavior of the copolymers. When the TDI/PHBV fraction is 7, compared to neat PHBV, the crystallinity of PHCN7 decreased to 55.5%, the melt crystallization temperature was increased to 77.9 °C, meanwhile the T_{max} increased by 48.5 °C. Furthermore, the copolymers became more hydrophobic (water contact angle 46°–60°) than neat CNCs. Most importantly, an efficient approach was presented to obtain the expected graft copolymers with the modulated crystallinity, good crystallization ability, better thermal stability, and favorable hydrophobicity and so on. Such copolymers exhibited great potential for their applications as nano reinforcing agents for hydrophobic polymer matrices and medical materials.

Acknowledgements

This work was supported by Top Priority Discipline of Zhejiang Provincial university, the Excellent Doctor Special Projects of Top Priority Provincial Discipline in Zhejiang Sci-Tech University (2013YBZX01), and Program for Department of Education of Zhejiang Province (Y201327880), the Scientific Research Foundation of Zhejiang Sci-Tech University (ZSTU) under Grant. No.13012069-Y, and the Natural Science Foundation of Zhejiang Province of China (LQ12C16005) as well as the Doctorate Innovation Foundation of Donghua University (BC201101).

Appendix A. Supplementary data

Supplementary material related to this article can be found, in the online version, at http://dx.doi.org/10.1016/j.carbpol.2013.09.048.

References

Angellier, H., Molina-Boisseau, S., Belgacem, M. N., & Dufresne, A. (2005). Surface chemical modification of waxy maize starch nanocrystals. *Langmuir, 21*, 2425–2433.

Bluhm, T. L., & Hamer, G. K. (1986). Studies of composition and crystallinity of bacterial poly(β-hydroxybutyrate-co-β-hydroxyvalerate). *Macromolecules*, *19*, 2865–2871.

Chen, G., Dufresne, A., Huang, J., & Chang, P. R. (2009). A novel thermoformable bionanocomposite based on cellulose nanocrystal-graft-poly(ε-caprolactone). *Macromolecular Materials and Engineering*, *294*, 59–67.

Chen, G. Q., & Wu, Q. (2005). The application of polyhydroxyalkanoates as tissue engineering materials. *Biomaterials*, *26*, 6565–6578.

Chen, Z., Cheng, S., & Xu, K. (2009). Block poly(ester–urethane)s based on poly(3-hydroxybutyrate-co-4-hydroxybutyrate) and poly(3-hydroxyhexanoate-co-3-hydroxyoctanoate). *Biomaterials*, *30*, 2219–2230.

Enomoto-Rogers, Y., Yoshinaga, H. K. A., & Takano, T. (2011). Synthesis of diblock copolymers with cellulose derivatives 4.Self-assembled nanoparticles of amphiphilic cellulosederivatives carrying a single pyrene group at the reducing-end. *Cellulose*, *18*, 1005–1014.

Habibi, Y., & Dufresne, A. (2008). Highly filled bionanocomposites from functionalized polysaccharide nanocrystals. *Biomacromolecules*, *9*, 1974–1980.

Habibi, Y., Goffin, A. L., Schiltz, N., Duquesne, E., Dubois, P., & Dufresne, A. (2008). Bionanocomposites based on poly(ε-caprolactone)-grafted cellulose nanocrystals by ring opening polymerization. *Journal of Materials Chemistry*, *18*, 5002–5010.

Habibi, Y., Lucia, L. A., & Rojas, O. J. (2010). Cellulose nanocrystals: Chemistry, self-assembly, and applications. *Chemical Reviews*, *110*, 3479–3500.

Hu, Y. J., Wei, X., Zhao, W., Liu, Y. S., & Chen, G. Q. (2009). Biocompatibility of poly(3-hydroxybutyrate-co-3-hydroxyvalerate-co-3-hydroxyhexanoate) with bone marrow mesenchymal stem cells. *Acta Biomaterialia*, *5*, 1115–1125.

Ke, Y., Wang, Y. J., Renb, L., Zhao, Q. C., & Huang, W. (2010). Modified PHBV scaffolds by in situ UV polymerization: Structural characteristic, mechanical properties and bone mesenchymal stem cell compatibility. *Acta Biomaterialia*, *6*, 1329–1336.

Klemm, D., Kramer, F., Moritz, S., Lindström, T., Ankerfors, M., Gray, D., & Dorris, A. (2011). Nanocelluloses: A new family of nature-based materials. *Angewandte Chemie International Edition*, *50*, 5438–5466.

Lao, H. K., Renard, E., Linossier, I., Langlois, V., & Vallée-Rehel, K. (2007). Modification of poly(3-hydroxybutyrate-co-3-hydroxyvalerate) film by chemical graft copolymerization. *Biomacromolecules*, *8*, 416–423.

Li, X., Liu, K. L., Wang, M., Wong, S. Y., Tjiu, W. C., He, C. B., Goh, S. H., & Li, J. (2009). Improving hydrophilicity, mechanical properties and biocompatibility of poly[(R)-3-hydroxybutyrate-co-(R)-3-hydroxyvalerate] through blending with poly[(R)-3-hydroxybutyrate]-alt-poly(ethylene oxide). *Acta Biomaterialia*, *5*, 2002–2012.

Lin, N., Huang, J., & Chang, P. R. (2011). Surface acetylation of cellulose nanocrystal and its reinforcing function in poly(lactic acid). *Carbohydrate Polymers*, *83*, 1834–1842.

Liu, Q. S., Shyr, T. W., Tung, C. H., Liu, Z., Shan, G., Zhu, M., & Deng, B. (2012). Particular thermal properties of poly(3-hydroxybutyrateco-3-hydroxyvalerate) oligomers. *Journal of Polymer Research*, *19*, 9756.

Liu, Q. S., Zhu, M. F., Wu, W. H., & Qin, Z. Y. (2009). Reducing the formation of six-membered ring ester during thermal degradation of biodegradable PHBV to enhance its thermal stability. *Polymer Degradation and Stability*, *94*, 18–24.

Lönnberg, H., Fogelström, L., Azizi-Samir, M. A. S. L. B., Malmström, E., & Hult, A. (2008). Surface grafting of microfibrillated cellulose with poly(ε-caprolactone)-Synthesis and characterization. *European Polymer Journal*, *44*, 2991–2997.

Menezes, A. J., Siqueira, G., Curvelo, A. S. A., & Dufresne, A. (2009). Extrusion and characterization of functionalized cellulose whiskers reinforced polyethylene nanocomposites. *Polymer*, *50*, 4552–4563.

Sato, H., Murakami, R., Padermshoke, A., Hirose, F., Senda, K., Noda, I., & Ozaki, Y. (2004). Infrared spectroscopy studies of CH. . .O hydrogen bondings and thermal behavior of biodegradable poly(hydroxyalkanoate). *Macromolecules*, *37*, 7203–7213.

Shang, W. L., Huang, J., Luo, H., Chang, P. R., Feng, J. W., & Xie, G. Y. (2013). Hydrophobic modification of cellulose nanocrystal via covalently grafting of castor oil. *Cellulose*, *20*, 179–190.

Taipina, M. O., Ferrarezi, M. M. F., Yoshida, I. V. P., & Gonçalves, M. C. (2013). Surface modification of cotton nanocrystals with a silane agent. *Cellulose*, *20*, 217–226.

Tehrani, A. D., & Neysi, E. (2013). Surface modification of cellulose nanowhisker throughout graft polymerization of 2-ethyle-2-oxazoline. *Carbohydrate Polymers*, *97*, 98–104.

Thielemans, W., Belacem, M. N., & Dufresne, A. (2006). Starch nanocrystals with large chain surface modifications. *Langmuir*, *22*, 4804–4810.

Viet, D., Beck-Candanedo, S., & Gray, D. G. (2007). Dispersion of cellulose nanocrystals in polar organic solvents. *Cellulose*, *14*, 109–113.

Wang, B., Liu, J., Zhang, J., Li, H., Chen, P., Gu, Q., & Wang, Z. (2013). Thermomechanical properties of the composite made of poly(3-hydroxybutyrate-co-3-hydroxyvalerate) and acetylated chitin nanocrystals. *Carbohydrate Polymers*, *95*, 100–106.

Wang, J., Wang, Z., Li, J., Wang, B., Liu, J., Chen, P., Miao, M., & Gu, Q. (2012). Chitin nanocrystals grafted with poly(3-hydroxybutyrate-co-3-hydroxyvalerate) and their effects on thermal behavior of PHBV. *Carbohydrate Polymers*, *87*, 784–789.

Yu, H. Y., Qin, Z. Y., Liang, B. L., Liu, N., Zhou, Z., & Chen, L. (2013). Facile extraction of thermally stable cellulose nanocrystals with a high yield of 93% through hydrochloric acid hydrolysis under hydrothermal conditions. *Journal of Materials Chemistry A*, *1*, 3938–3944.

Yu, H. Y., Qin, Z. Y., Liu, Y. N., Chen, L., Liu, N., & Zhou, Z. (2012). Simultaneous improvement of mechanical properties and thermal stability of bacterial polyester by cellulose nanocrystals. *Carbohydrate Polymers*, *89*, 971–978.

Yu, H. Y., Qin, Z. Y., Wang, L. F., & Zhou, Z. (2012). Crystallization behavior and thermal properties of biodegradable ethyl cellulose-g-poly(3-hydroxybutyrate-co-3-hydroxyvalerate): The influence of the length and grafting density of the crystallizing side chains. *Carbohydrate Polymers*, *87*, 2447–2454.

Zhu, J., Dong, X. T., Wang, X. L., & Wang, Y. Z. (2010). Preparation and properties of a novel biodegradable ethyl cellulose grafting copolymer with poly(p-dioxanone) side-chains. *Carbohydrate Polymers*, *80*, 350–359.